Pharm Res (2013) 30:1188–1199
DOI 10.1007/s11095-012-0956-5

RESEARCH PAPER

Mechanistic Modeling to Predict the Transporter- and Enzyme-Mediated Drug-Drug Interactions of Repaglinide

Manthena V. S. Varma • Yurong Lai • Emi Kimoto • Theunis C. Goosen • Ayman F. El-Kattan • Vikas Kumar

Received: 13 August 2012 / Accepted: 6 December 2012 / Published online: 10 January 2013

ABSTRACT

Purpose Quantitative prediction of complex drug-drug interactions (DDIs) is challenging. Repaglinide is mainly metabolized by cytochrome-P-450 (CYP)2C8 and CYP3A4, and is also a substrate of organic anion transporting polypeptide (OATP)1B1. The purpose is to develop a physiologically based pharmacokinetic (PBPK) model to predict the pharmacokinetics and DDIs of repaglinide.

Methods *In vitro* hepatic transport of repaglinide, gemfibrozil and gemfibrozil 1-*O*-β-glucuronide was characterized using sandwich-culture human hepatocytes. A PBPK model, implemented in Simcyp (Sheffield, UK), was developed utilizing *in vitro* transport and metabolic clearance data.

Results *In vitro* studies suggested significant active hepatic uptake of repaglinide. Mechanistic model adequately described repaglinide pharmacokinetics, and successfully predicted DDIs with several OATP1B1 and CYP3A4 inhibitors (<10% error). Furthermore, repaglinide-gemfibrozil interaction at therapeutic dose was closely predicted using *in vitro* fraction metabolism for CYP2C8 (0.71), when primarily considering reversible inhibition of OATP1B1 and mechanism-based inactivation of CYP2C8 by gemfibrozil and gemfibrozil 1-*O*-β-glucuronide.

Conclusions This study demonstrated that hepatic uptake is rate-determining in the systemic clearance of repaglinide. The model quantitatively predicted several repaglinide DDIs, including the complex interactions with gemfibrozil. Both OATP1B1 and CYP2C8 inhibition contribute significantly to repaglinide-gemfibrozil interaction, and need to be considered for quantitative rationalization of DDIs with either drug.

Electronic supplementary material The online version of this article (doi:10.1007/s11095-012-0956-5) contains supplementary material, which is available to authorized users.

M. V. S. Varma (✉) • Y. Lai • E. Kimoto • T. C. Goosen • A. F. El-Kattan
Pharmacokinetcis, Dynamics and Metabolism, Pfizer Inc.
Groton, Connecticut, USA
e-mail: manthena.v.varma@pfizer.com

V. Kumar
Clincial Pharmacology, Pfizer Inc., Groton, Connecticut, USA

KEY WORDS CYP2C8 · drug-drug interaction · gemfibrozil · OATP1B1 · physiologically-based pharmacokinetic model · repaglinide

INTRODUCTION

Serious side-effects caused by drug-drug interactions (DDIs) could be unmanageable in clinic and may lead to market withdrawals. For example, cerivastatin was withdrawn because of higher incidences of rhabdomyolysis in the patients concomitantly dosed with gemfibrozil (1). Consequently, the ability to predict DDIs early in drug development is essential to minimize the clinical risks associated with drug interactions. Confidence in the prediction of DDIs for drugs cleared via cytochrome-P-450 (CYP) enzymes is generally high (2,3). However, approaches for the quantitative prediction of transporter-based DDIs are not well established. In addition, significant challenges arise in the evaluation and/or prediction of complex drug interactions caused by inhibitor drugs that affect both transporter- and enzyme-mediated disposition (4,5). The US Food and Drug Administration (USFDA) and European Medicines Agency (EMA) recently issued draft guidance for pharmaceutical industry, which provided recommendations for the *in vitro* and *in vivo* evaluation of transporter- and enzyme-based DDI (6–8). Furthermore, regulators suggest use of mechanistic physiologically-based pharmacokinetic (PBPK) modeling to quantitatively predict the magnitude of DDIs in various clinical situations (7,9).

Repaglinide, an oral anti-diabetic agent (10), is majorly metabolized by CYP2C8 and CYP3A4, and is also a substrate to hepatic uptake transporter, organic anion transporter polypeptide (OATP)1B1 (5,11–13). Oxidative biotransformation of repaglinide by both CYP2C8 and CYP3A4 has been reported *in vitro* (11–13), but their relative contribution *in vivo* is unclear. On the basis of recent clinical DDIs studies, an apparent *in vitro-in vivo* disconnect in the

fraction metabolism of the two CYPs has been suggested (14,15). Pharmacogenomic studies demonstrated an association between repaglinide exposure and genetic polymorphisms in *SLCO1B1* and *CYP2C8* (16,17), indicating the significance of both mechanisms in determining the systemic clearance of repaglinide. However, the relative importance of hepatic uptake and metabolism in its hepatic elimination *in vivo* is not well understood.

Repaglinide show significant DDIs with several inhibitory drugs (18). Notably, gemfibrozil caused up to 8.3-fold increase in the area under the plasma concentration-time curve (AUC) of repaglinide (14). Gemfibrozil dosing leads to CYP2C8 inhibition *in vivo*, which is thought to be mainly due to mechanism-based inactivation of CYP2C8 by its major circulating metabolite, gemfibrozil 1-*O*-β-glucuronide (19). *In vitro*, both parent and metabolite also inhibit OATP1B1, and weakly inhibit CYP3A4 (20,21). In general, the phenomena observed *in vivo* suggest the repaglinide-gemfibrozil interaction could be a complex DDI involving inhibition of multiple processes caused by both gemfibrozil and gemfibrozil 1-*O*-β-glucuronide; and would be challenging to quantitatively predict using static models (4,5,14,15). The aim of this work was to develop a comprehensive mechanistic (whole-body PBPK) model of repaglinide, utilizing the hepatic transport (sinusoidal active uptake, passive diffusion and canalicular efflux) and metabolic intrinsic clearance values obtained from *in vitro* studies. The mechanistic model was used to simulate the plasma concentration-time profiles and further assess the transporter- and/or enzyme-mediated clinical DDIs of repaglinide.

MATERIALS AND METHODS

Materials

Cryopreserved human hepatocytes lot BD310 was purchased from BD Biosciences (Woburn, MA, USA). Gemfibrozil and rifamycin SV were purchased from Sigma (St. Louis, MO). Gemfibrozil 1-O-β-glucuronide was purchased from Toronto Research Chemicals Inc. (Ontario, Canada). Media for hepatocyte culture including *In Vitro*Gro-HT (thawing), *In Vitro*Gro-CP (plating) and *In Vitro*Gro-HI (incubation) supplemented with Torpedo Antibiotic Mix were from Celsis *In Vitro* Technologies (Baltimore, MD). BioCoat 24-well plates and Matrigel were procured from BD Biosciences (Bedford, MA).

Transport Studies Using Sandwich Culture Human Hepatocyte (SCHH) Model

Cryopreserved hepatocytes were thawed and plated with cell density of 0.75×10^6 cells/mL as described previously (22). For hepatic uptake study in SCHH, the hepatocytes were pre-incubated for 10 min in the absence or presence of 100 μM rifamycin SV in Hanks' balanced salt solution (HBSS) or with Ca^{2+}/Mg^{2+} free HBSS, at 37°C. After aspirating the pre-incubation buffer, the hepatic uptake was initiated by adding 0.5 mL of incubation buffer containing substrates (1 μmol/L) with and without rifamycin SV. The uptake was terminated at a designated time by adding 0.5 mL of ice cold HBSS buffer after removal of the incubation buffer. The substrates were extracted by methanol containing internal standard for LC-MS/MS quantification. The hepatic uptake rates were calculated from the linear regression of the initial time points.

Analysis of samples were conducted by LC-MS/MS on an API-4000 triple quadrupole mass spectrometer (Applied Biosystem, Foster City, CA), with atmospheric pressure electrospray ionization source (MDS-SCIEX, Concord, Ontario, Canada). Samples (10 μL) were injected onto a Aquasil-C18 column (2.1 × 30 mm, 3.0 μ; Thermo Fisher Scientific) and eluted by a mobile phase with initial conditions of 5% solvent B, followed by a linear gradient of 5% solvent B to 30% solvent B over 5 min (solvent A: 100% water with 0.1% formic acid; solvent B: 100% acetonitrile with 0.1% formic acid) at a flow rate of 0.4 mL/min.

Pharmacokinetic Modeling and Simulations

Whole-body PBPK modeling and simulations of clinical pharmacokinetics and drug-drug interactions were performed using the population-based ADME simulator, Simcyp (version 11.0, SimCYP Ltd, Sheffield, UK). Each simulation was performed for 50 subjects (5 trials × 10 subjects). The virtual populations of healthy subjects had a body weight of 70 kg, with age ranging from 18 to 65 years, and included both sexes. Dose, dosing interval, and dosing duration of repaglinide in control and treatment cohorts is identical to that reported in individual clinical studies.

Repaglinide Model Development

Repaglinide model was built using the physicochemical properties, *in vitro* preclinical data such as human plasma fu, blood-to-plasma ratio, metabolic intrinsic clearance values, *etc.* (Table I). Full-PBPK model using Rodgers *et al.* method (23,24) considering rapid equilibrium between blood and tissues was adopted to obtain the distribution of repaglinide into all organs, except liver. Permeability-limiting distribution of repaglinide into liver was considered, for which, sinusoidal active uptake intrinsic clearance and passive diffusion obtained from SCHH studies, were incorporated to capture hepatic disposition (Supplementary Material Figure S1). A scaling factor for the active uptake intrinsic clearance, which was initially assumed as one, was estimated by optimizing using intravenous plasma concentration-time profile, while fixing the

Table I Summary of Input Parameters for Repaglinide PBPK Model

Parameters	Repaglinide	Source
Physicochemical properties		
Molecular weight (g/mol)	452.6	ACD
log P	4.87	ACD
Compound type	Ampholyte	ACD
pK_a	4.19 & 5.78	ACD
Fraction unbound	0.015	(53)
Blood/plasma ratio	0.62	(12)
Absorption		
Absorption type	ADAM	
Fraction absorbed	>0.95	(54)
Caco-2 permeability ($\times 10^{-6}$cm/s)	26.1	In-house data
Absorption Scalar	1.873	In-house data
fuGut	1	Assumed
Distribution		
Distribution model	Whole-body PBPK	(Rodgers *et al.*) (23,24)
Elimination		
$Cl_{int,\ met}$ (μL/min/mg)	131	(12,29)
fm_{CYP2C8}	0.71	(12)
Urinary excretion	<1%	(50)
Hepatobiliary transport		
Liver unbound fraction (Intra-/extra-cellular)	0.143/0.028	Calculated
Passive diffusion (μL/min/10^{-6}cells)	24	SCHH data
$CL_{int,active}$ (μL/min/10^{-6}cells)	37	SCHH data
Scaling factor (Active uptake)	16.9	Estimated[a]
$CL_{int,efflux}$ (μL/min/10^{-6}cells)	0	SCHH data

[a] Estimated by fitting to intravenous pharmacokinetics data. See Methods

ACD Calculated using Advanced Chemistry Development (ACD/Labs) Software V11.02. (SciFinder 2007.1)

ADAM Advanced dissolution, absorption and metabolism model; *P* partition coefficient; pK_a acid dissociation constant

rest of the parameters (25,26). Absorption phase in the model was captured by advanced dissolution, absorption and metabolism (ADAM) model using Caco-2 permeability data.

Inhibitor Drug Models

A perfusion-limited model of gemfibrozil was developed using clinical first-order absorption rate, Fa, volume of distribution and total clearance (Table II). About 79% of the gemfibrozil is metabolized by UGTs to form gemfibrozil 1-*O*-β-glucuronide *in vitro*, while the rest undergoes oxidative metabolism by CYP3A4 (27). Lag-time of 15 min was considered for oral absorption (25). A model for gemfibrozil 1-*O*-β-glucuronide was build based on metabolite formation rate from gemfibrozil (fm 0.79), fu and blood/plasma ratio. Due to the lack of data, the Vss (0.1 L/h) and biliary intrinsic clearance (3.8 µL/min/10^6cells) for the metabolite were estimated (assuming complete elimination via bile), by "retrograde" fitting to the observed plasma concentration-time profile assuming perfusion-limited disposition. Input parameters for cyclosporine were previously reported (25). Models for clarithromycin, ketoconazole and itraconazole are available in the Simcyp compound library, and were directly adopted (input parameters, Table II).

RESULTS

In Vitro Hepatobiliary Transport

SCHH studies in the absence and presence of rifamycin SV or calcium yielded intrinsic clearance (CL_{int}) values for sinusoidal active uptake ($CL_{int,active}$), passive diffusion (CL_{pd}) and canalicular efflux ($CL_{int,efflux}$) of 37±8.1, 24±6.4 and 0.1±0 µl/min/10^6cells, respectively (Table I). The higher uptake clearance ($CL_{int,uptake}=CL_{int,active}+CL_{pd}$), as compared to passive diffusion suggest need for a permeability-limited model to capture hepatic disposition of repaglinide (25,26,28).

Repaglinide Pharmacokinetics

Considering permeability-limited hepatic disposition, *in vitro* intrinsic clearance values of hepatic transport and metabolism along with other input parameters (listed in Table I), were used to build the whole-body PBPK (Simcyp) model for repaglinide (Supplementary Material Figure S1). The human liver microsomal intrinsic clearance ($CL_{int,met}$) and the fraction metabolism contribution of CYP2C8 to the total metabolic clearance (fm_{CYP2C8}) used in the model are 131 µl/min/mg-microsomal protein and 0.71, respectively (12,29). However, PBPK model with these initial parameters overpredicted the intravenous plasma concentration-time profile (Figure 1). Interestingly, repaglinide plasma exposure was found to be relatively less sensitive to changes in metabolic clearance. Accordingly, alteration of the $CL_{int,met}$ by as much as 100-fold did not recover the observed intravenous pharmacokinetic profile (Supplementary Material Figure S2). Overall, the simulations with the initial parameters suggest an apparent *in vitro–in vivo* disconnect in the hepatic uptake rate. Therefore, an empirical scaling factor was applied for the hepatic sinusoidal active uptake (SF_{active} – 16.9), which was obtained by fitting the model to the intravenous data (25,26), while fixing the other input parameters, (Figure 1). Depending on the experimental systems applied, wide range of estimates for the microsomal CL_{int} were reported (11–13,29). In sensitivity analysis of $CL_{int,met}$, the estimated SF_{active} was found to be about 12 and 32 when the $CL_{int,met}$ was altered to 393 (3X) and 39.3 µl/min/mg (0.3X), respectively.

Table II Summary of Input Parameters for the Models of the Perpetrator Drugs.

Parameters	Gemfibrozil[a]	Gemfibrozil 1-O-β-glucuronide[b]	Cyclosporine[a]	Ketoconazole[c]	Itraconazole[c]	Clarithromycin[c]
Physicochemical properties						
Molecular weight (g/mol)	250.3	426.5	1202.6	531.4	705.6	748
log P/Log $D_{7.4}$	4.3	3.3	2.78	4.04	5.66	1.7
Compound type	Monoprotic acid	Monoprotic acid	Neutral	Diprotic base	Monoprotic base	Monoprotic base
pK_a	4.75	2.68	-	2.9 & 6.5	3.7	8.99
Fraction unbound	0.03	0.115 (20)	0.068	0.029	0.036	0.18
Blood/plasma ratio	0.825	0.825	1.36	0.62	0.58	1.0
Absorption						
Absorption type	First-order		First-order	First-order	First-order	First-order
Fraction absorbed	1.0		0.86	1.0	1.0	1.0
Absorption rate constant (1/h)	3.0		1.50	1.9	0.62	2.37
fuGut	1.0		1.0	0.06	0.016	1.0
Distribution						
Distribution model	Minimal PBPK	Minimal PBPK	Full PBPK (Polin and Theil)	Minimal PBPK	Minimal PBPK	Minimal PBPK
Vss (L/kg)	0.13	0.1[d]		0.345	10.7	1.75
Elimination						
Total Clearance IV/PO (L/h)	7.12 (PO)		27.7 (IV)	13.8 (PO)	22.9 (IV)	31.14 (IV)
fm_{UGT}	0.79 (others)					
fm_{CYP3A4}	0.21 (CYP3A4)					
CLint Biliary (μL/min/10^6 cells)		3.8[d]				
Renal Clearance (L/h)				0.13		8.05
Inhibition potency						
fu,mic	0.74	0.78	0.89	0.97	1.0	1.0
CYP2C8 Ki (μmol/l)	9.3	(10.1 & 12.6)[e]		2.5		
CYP3A4 Ki (μmol/l) (2.47 & 2.94)[f]	92	133	0.34	0.015	0.0013	2.43
OATP1B1 Ki (μmol/l)	2.52	7.9	0.014			

When only IC_{50} value was reported, Ki was assumed to be $IC_{50}/2$

[a] Input parameters taken from references (25)

[b] Physicochemical properties were calculated using Advanced Chemistry Development (ACD/Labs) Software V11.02. Blood/plasma ratio was assumed to be similar to that gemfibrozil

[c] Input parameters were directly adopted from compound files of Simcyp compound library (42)

[d] Value was selected based on best fit to the pharmacokinetic profiles

[e] Values represent mechanism-based inactivation parameters (KI μmol/l and Kinact 1/h) of gemfibrozil 1-O-β-glucuronide (19,40)

[f] Values represent mechanism-based inactivation parameters (KI μmol/l and Kinact 1/h) of clarithromycin (55,56)

The ADAM model was used to capture intestinal absorption and predict oral pharmacokinetics of repaglinide (Figure 2). In general, the mechanistic model adequately described repaglinide oral pharmacokinetics at three different doses obtained from eight separate clinical studies (30–38). However, the data from separate clinical studies inherited considerable variability in the maximum plasma concentration (Cmax) (32,39); and the model appeared to underpredict Cmax, particularly at 0.25 mg dose (Figure 2a). Sensitivity analysis was performed to assess the influence of input parameters on the repaglinide systemic and hepatic exposure after oral dosing (Supplementary Material Figure S3). Notably, $CL_{int,active}$ showed prominent effect on the systemic exposure, but did not have an effect on the hepatic exposure. In contrast, $CL_{int,CYP2C8}$ and $CL_{int,CYP3A4}$ showed a relatively small effect on the systemic exposure, while significantly influencing the hepatic exposure. Other input parameters such as intestinal permeability, $f_{u,gut}$ and CL_{pd} had minimum or no effect on both systemic and hepatic exposure.

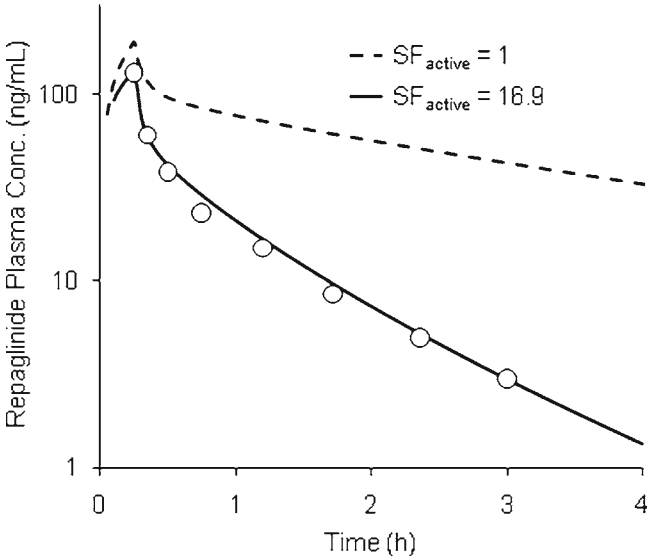

Fig. 1 Model simulations of repaglinide plasma concentration-time profiles after intravenous infusion of 2.0 mg dose, without and with scaling factor for active hepatic uptake intrinsic clearance. Data points represent mean observed values (30). Average percentage prediction error (PPE= 100x|(predicted-observed)/observed|) of AUC is >300% and 8% with SF_{active} of 1 and 16.9, respectively.

Drug-Drug Interaction Predictions

Models for gemfibrozil and its major circulating metabolite, gemfibrozil 1-*O*-β-glucuronide, were developed using *in vitro* and *in vivo* input parameters (Table II). Simulated plasma concentration-time profiles for both gemfibrozil and gemfibrozil 1-*O*-β-glucuronide were similar to that observed *in vivo* (Figure 3). For DDI predictions, gemfibrozil was considered to reversibly inhibit OATP1B1 (Ki – 2.52 μmol/l) (25), CYP2C8 (Ki – 9.3 μmol/l) (40) and CYP3A4 (Ki – 92 μmol/l) (21) metabolism, while its major circulating metabolite, gemfibrozil 1-*O*-β-glucuronide, also exerted inhibition on OATP1B1 (Ki – 7.9 μmol/l) (41) and CYP3A4 (Ki – 133 μmol/l) (20), along with mechanism-based inactivation of CYP2C8 (KI – 10.1 μmol/l; Kinact – 12.6 1/h) (19,40).

Repaglinide-gemfibrozil interactions were initially simulated considering *in vitro* fm_{CYP2C8} (0.71) and $CL_{int,met}$ (131 μl/min/mg) (12,29). Using the reported *in vitro* interaction parameters, model well predicted the complex repaglinide-gemfibrozil interaction following single and multiple therapeutic doses of gemfibrozil (600-900 mg) (Figure 4a). Further delineation of interaction, by assuming only OATP1B1 or CYPs inhibition, suggested that inhibition of both transporter- and enzyme-mediated disposition contributed equally to the predicted interaction at the gemfibrozil therapeutic dose. CYP2C8 inhibition recovered only <3-fold AUC ratio, which appeared to be the maximum at 300 mg gemfibrozil. Despite accurate predictions at therapeutic dose, the model slightly underpredicted gemfibrozil dose- and time-dependent interactions (Figure 4a and b). For instance, model underpredicted DDI with single gemfibrozil subtherapeutic (100 mg and 300 mg) dose administered 1 h before the repaglinide oral dosing (14). Also, the model predictions were lower than the observed values when repaglinide was administered ≥3 h after the gemfibrozil (600 mg) dose (34).

Further sensitivity analyses were conducted to evaluate model performace for repaglinide-gemfibrozil interactions. First, sensitivity analysis of the *in vitro* mechanism-based inactivation parameters (K_{inact} and KI) (19,40) or the CYP2C8 degradation half-life (8-41 h) (3) did not recover the differences in the model predicted and the observed AUC ratios. Second, a wide range of values for repaglinide intrinsic metabolic clearance are reported (11–13), and the model showed increase in AUC ratio with the decrease in $CL_{int,met}$ value, while fixing the fm_{CYP2C8} to 0.71 (Figure 4). Interestingly, model using 0.3X $CL_{int,met}$ well predicted DDIs with gemfibrozil at its sub-therapeutic doses and also the later part of time-dependent interaction, however, over-predicting interaction with concomitant dosing of therapeutic dose (Figure 4b and d). Similar trend was noted for the prediction of repaglinide exposure when the drug is ingested after the last dose of multiple gemfibrozil doses (15,35) (data not shown).

Established models for inhibitor drugs, including cyclosporine, ketoconazole, clarithromycin and itraconazole were used to predict repaglinide DDIs (Table II) (25,42). Repaglinide DDIs with CYP3A4 inhibitor drugs (clarithromycin, ketoconazole and itraconazole) and OATP1B1 inhibitor drug (cyclosporine) are well predicted by the final model of repaglinide (Figure 5). Furthermore, the model predicted the AUC increase (predicted ~17-fold Vs observed ~19-fold), as well as the plasma concentration-time profile of repaglinide when dosed in combination with gemfibrozil and itraconazole (Figures 5 and 6) (39). Based on the average percentage prediction error (PPE=100x|(predicted-observed)/observed|) of all the above noted DDI predictions (Figure 5), the final PBPK model of repaglinide yielded very close predictions (average PPE ~ 7%).

Active Hepatic Uptake of Gemfibrozil and Gemfibrozil 1-*O*-β-glucuronide

SCHH studies showed significantly ($p<0.05$) reduced uptake of both the gemfibrozil and gemfibrozil 1-*O*-β-glucuronide in the presence of rifamycin SV, suggesting active hepatic uptake (Figure 7). The uptake clearance was ~1.5- and 3-fold higher than passive diffusion for the parent and metabolite, respectively. Furthermore, hepatocyte accumulation of metabolite is ~10-fold higher following incubation with gemfibrozil, as compared to incubation with metabolite in the presence of rifamycin SV (absence of active transport).

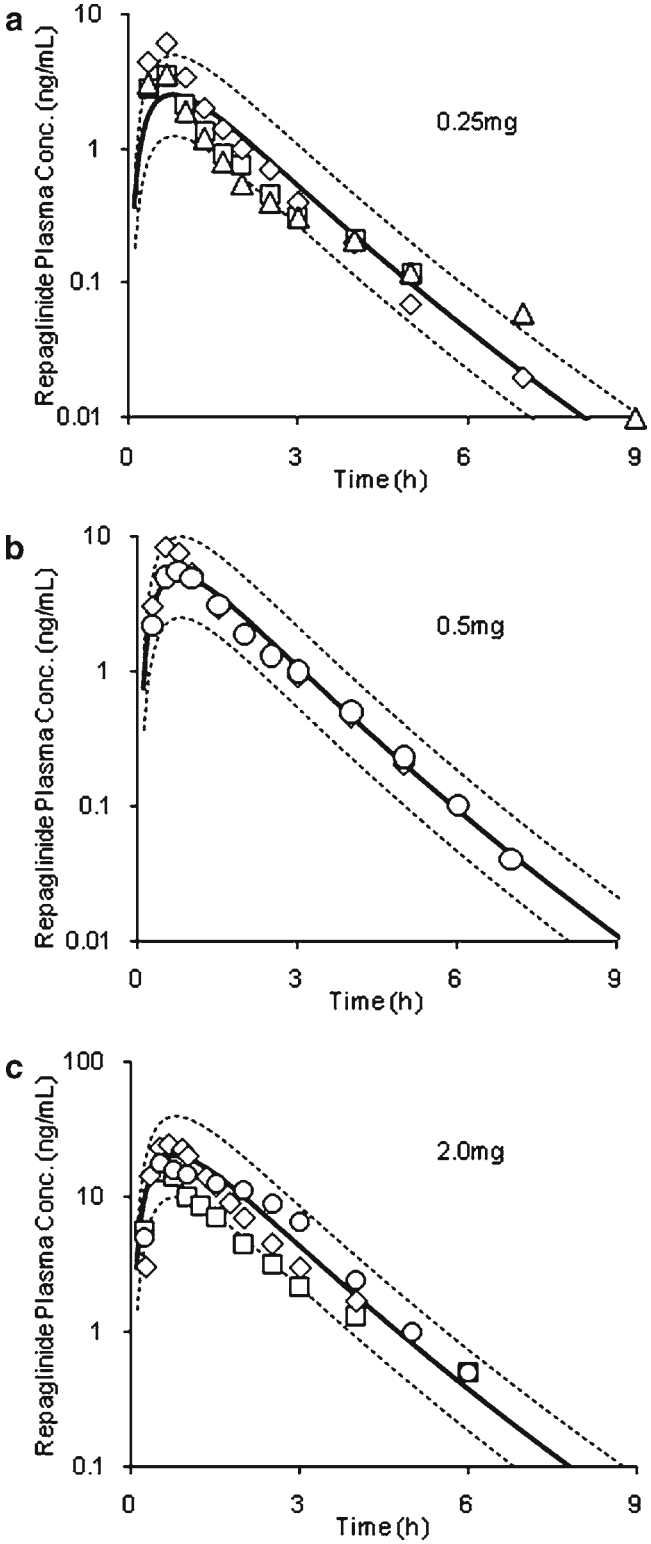

Fig. 2 Model simulations of repaglinide plasma concentration-time profiles following oral administration of (**a**) 0.25 mg, (**b**) 0.5 mg, and (**c**) 2.0 mg dose. *Solid* and *dotted lines* represent mean and 2-fold boundary of model simulations, respectively. Different data symbols represent mean observed values from separate clinical studies (30–38).

DISCUSSION

Repaglinide is mainly metabolized by CYP2C8 and CYP3A4 to its major oxidative metabolites, and to a minor extent by direct glucuronidation (11–13). Several preclinical and clinical studies also suggested that OATP1B1-mediated sinusoidal uptake plays a major role in the disposition of repaglinide (17,32). Consequently, complex DDIs are anticipated when repaglinide is dosed in combination with drugs affecting these multiple processes. In this study, we characterized the hepatic transport of repaglinide using SCHH model, and developed a mechanistic model to predict its pharmacokinetics and DDIs.

In vitro estimates of hepatic transport and metabolic intrinsic clearances indicate that uptake rate is higher than the passive diffusion, and also passive diffusion is lower than the total metabolic intrinsic clearance, suggesting that hepatic uptake is the rate-determining step in the overall clearance of repaglinide. This is further reflected in the PBPK model simulations, where the intravenous as well as oral plasma concentration-time profiles of repaglinide are in good agreement with the observed data when considering significant hepatic active uptake clearance (Figures 1 and 2). Our findings are consistent with a previous PBPK model, which also suggested permeability-limited hepatic disposition of repaglinide (43). Collectively, the systemic clearance of repaglinide is determined mainly by the hepatic uptake process.

The initial model, which directly used *in vitro* transport parameters underpredicted repaglinide systemic clearance, and therefore, an empirical scaling factor for $CL_{int,active}$–estimated by a "top-down" fitting to human intravenous plasma concentration-time profile (25,26)–was incorporated in the model (Figure 1). Previous PBPK approaches also suggest the need for empirical scaling factors applied to hepatic active uptake to recover human pharmacokinetics of several OATP substrates (25,26,44). The apparent discrepancy in the *in vitro-in vivo* extrapolation of active uptake and the compulsion for a scaling factor can be explained in part by the differences in transporter abundance in the *in vitro* (SCHH) and *in vivo* systems. Emerging proteomics data from our laboratory indicated that the OATP1B1 protein content of the human hepatocyte membrane is about two-fold higher than that quantified in SCHH (45). However, based on our previous and present studies, the SF_{active} derived by the "top-down" approach seems to be compound-specific (25,26), suggesting the differences in transporter expression levels may only partially bridge the gap. Additionally, the estimated SF_{active} for repaglinide was found to be partly dependent on the metabolic clearance input values – when evaluated within the reported range (12,13,29). On the other hand, potential active uptake into other tissues may also contribute to repaglinide disposition (46,47). Further understanding in these areas is necessary to

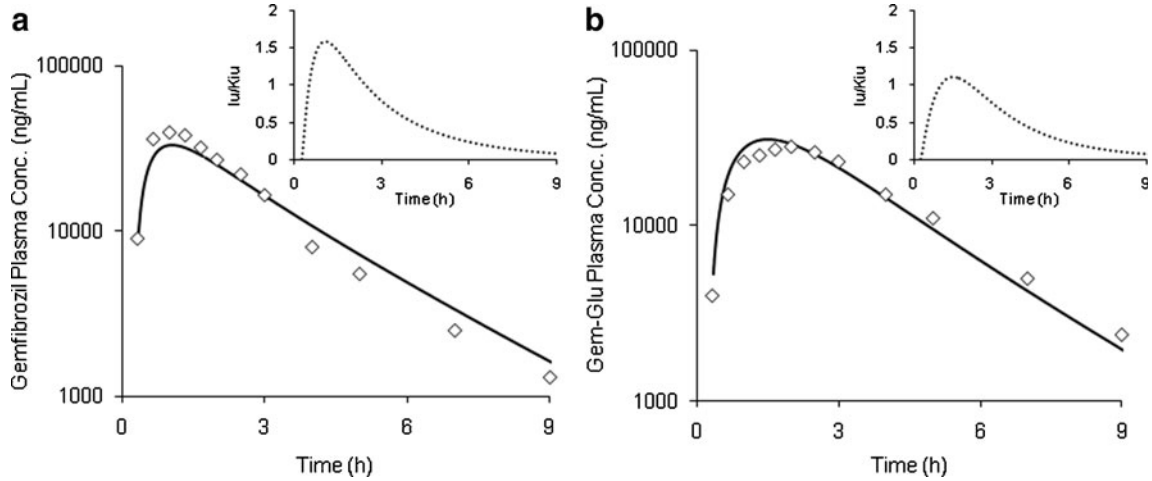

Fig. 3 Plasma concentration-time profiles of (**a**) gemfibrozil and (**b**) gemfibrozil 1-*O*-β-glucuronide, after oral administration of 600 mg dose. *Solid lines* represent mean simulation profiles. Data points represent mean observed values taken from literature (35). Insert shows the OATP1B1 reversible inhibitory potency-time profiles of gemfibrozil and its metabolite.

rationalize the assumptions and further validate or refine the current model.

The mechanistic model closely predicted the complex-DDI with gemfibrozil, at therapeutic dose (600 mg), when primarily considering reversible inhibition of OATP1B1 by both gemfibrozil and gemfibrozil 1-*O*-β-glucuronide, and mechanism-based inactivation of CYP2C8 by gemfibrozil 1-*O*-β-glucuronide. The interaction of repaglinide with CYP3A4 inhibitors is rather small, which was noted in the drug interaction studies with clarithromycin, itraconazole and ketoconazole (Figures 5 and 6). Nevertheless, concomitant use of repaglinide with drug-combinations inhibiting OATP1B1, CYP2C8 and CYP3A4 could lead to hazardous interactions. This is particularly evident with about 19-fold increase in repaglinide AUC when dosed in combination with itraconazole and gemfibrozil (39). Simulations showed a similar magnitude of interaction, thereby corroborating the involvement of complex drug interaction combining reversible and mechanism-based inactivation of CYP2C8 and reversible inhibition of CYP3A4 and OATP1B1.

Despite predicting the complex DDI of repaglinide with gemfibrozil—at its therapeutic dose and above (600–900 mg)—the mechanistic model, slightly underpredicted dose-dependent interactions at subtherapeutic doses (Figure 4a). We hypothesized that gemfibrozil and/or 1-*O*-β-glucuronide may accumulate in the hepatocytes to high concentrations, required for complete inhibition or inactivation of CYP2C8 activity even at subtherapeutic doses. Our *in vitro* SCHH studies suggested that the concentrations of gemfibrozil and 1-*O*-β-glucuronide in the liver would be much higher than predicted by the current inhibitor (and metabolite) model, which assumed perfusion-limited distribution (Figure 7). Recent studies also demonstrated non-linear systemic exposure for both gemfibrozil and gemfibrozil 1-*O*-β-glucuronide, with increased AUC at high doses (14,15). Collectively, this suggests involvement of saturable transporter-mediated hepatic disposition for the drug and metabolite. Based on the current model, CYP2C8 activity is not completely inhibited at lower doses (Supplementary Material Figure S4). Thus, underprediction of the interaction at subtherapeutic doses of gemfibrozil may be partially attributable to underestimation of hepatic concentrations of gemfibrozil 1-*O*-β-glucuronide, in particular. Further extrapolation of the metabolite hepatic exposure and incorporation of model components to capture active hepatic accumulation may be needed to evaluate the possible role of higher hepatic concentrations on AUC changes at subtherapeutic doses of gemfibrozil.

Similarly, the mechanistic model also slightly underpredicted *in vivo* time-dependent inhibition by gemfibrozil, when it was separated from repaglinide dosing by 3 or more hours (Figure 4c). Sensitivity analysis of CYP2C8 mechanism-based inactivation parameters (KI, K_{inact} and K_{deg}) did not show any improvement in predictions. The potential reasons for underprediction of dose- and time-dependent interactions include one or a combination of the following: (i) high and sustained concentrations of gemfibrozil 1-*O*-β-glucuronide in the liver relative to the plasma may cause prolonged inhibition of CYP2C8 and possibly CYP3A4, (ii) possible lower intrinsic metabolic clearance of repaglinide than used in the current model (Figure 4b and d), and (iii) potent and prolonged OATP1B1 inhibition by gemfibrozil and its metabolites *in vivo*. For reasons that are not clearly known, cyclosporine shows a long-lasting inhibitory effect on OATP1B1 and OATP1B3, and with relatively potent inhibition (low Ki) on co-incubation following a pre-incubation phase (48,49). Further understanding in these areas is warranted.

One of the distinct observations is the change in predicted AUC ratios as a function of metabolic intrinsic

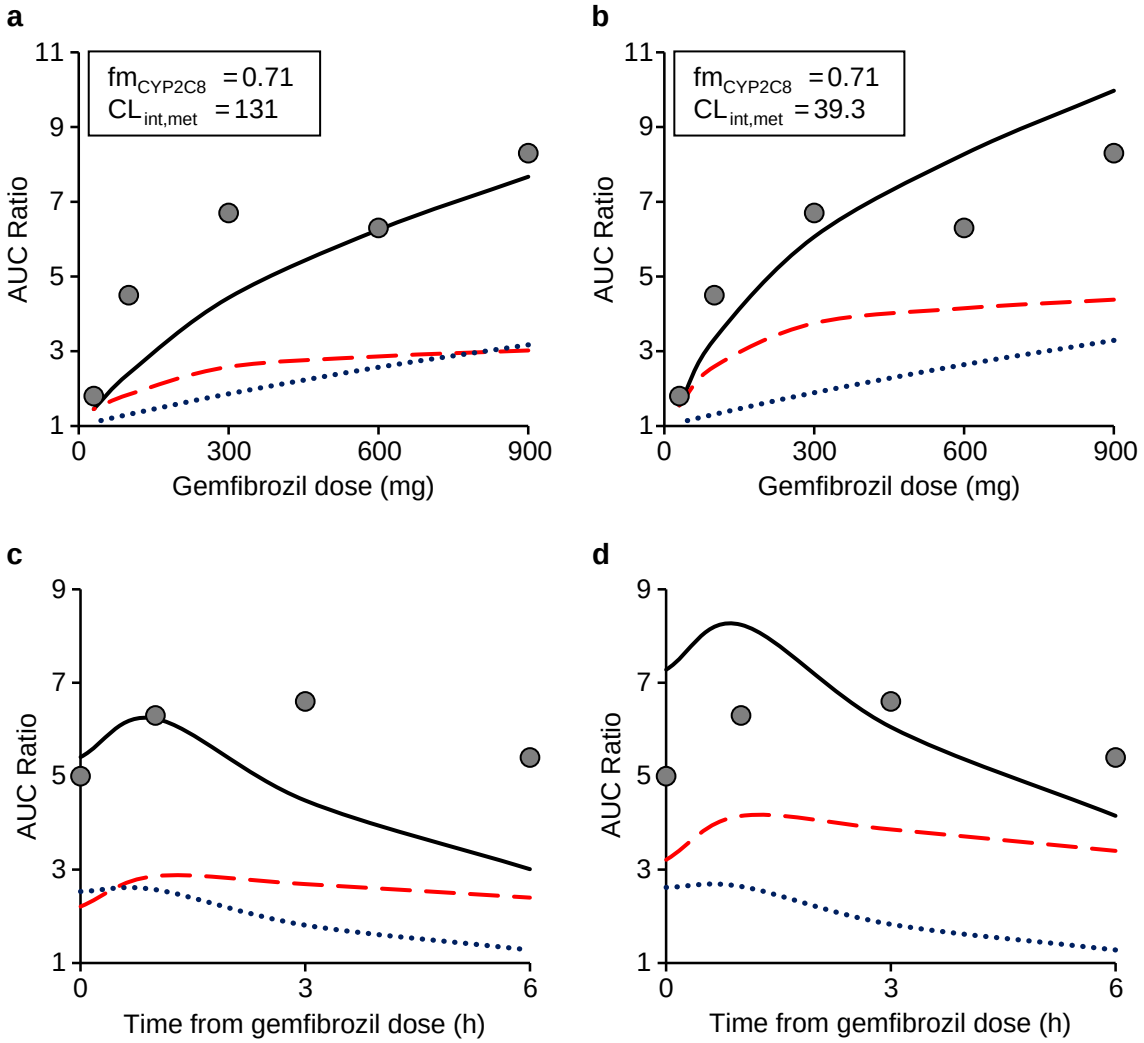

Fig. 4 Model predictions of repaglinide-gemfibrozil dose- and time-dependent interactions. Effect of repaglinide $CL_{int,met}$ on the predictions of dose- (**a** and **b**) and time-dependent (**c** and **d**) interactions after a single dose of gemfibrozil. In case of time-dependent studies gemfibrozil dose is 600 mg. Curves represent model predicted mean AUC ratios assuming inhibition of only OATP1B1 (*dotted*), only CYPs (*dashed*) and both (*solid*). Filled data points represent mean AUC ratios observed clinically (14,34). For simulations, dosage regimen of repaglinide and gemfibrozil was similar to the original reported study design.

Fig. 5 Observed and model predicted AUC ratios of repaglinide drug-drug interactions. Observed AUC ratios were taken from separate clinical studies (14,32–34,36,39). For simulations, dosage regimen of the inhibitor drugs and repaglinide is similar to the original reported study design. Average percentage prediction error (PPE=100x|(predicted-observed)/observed|) of AUC ratio is 7%.

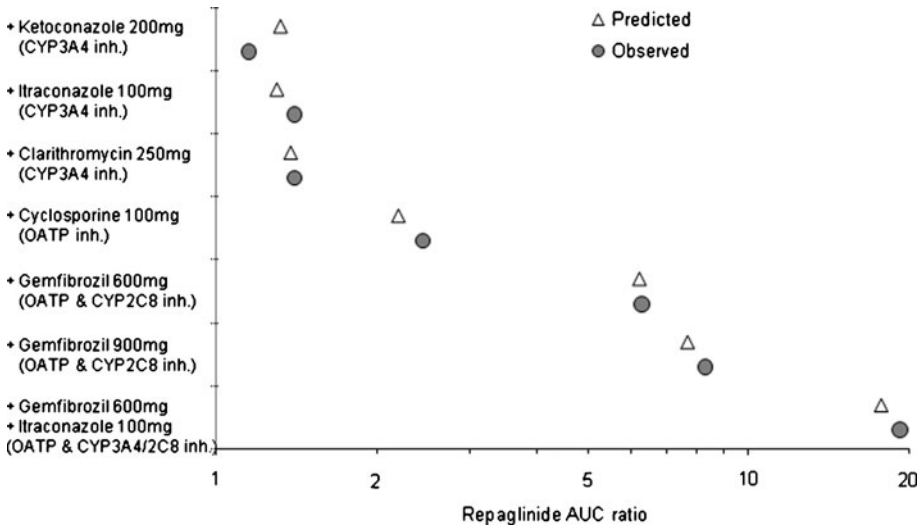

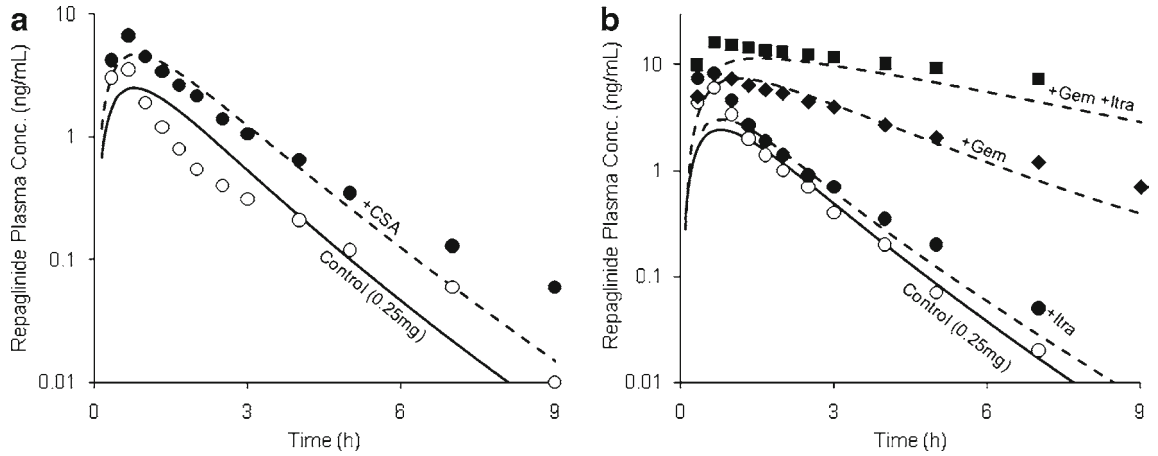

Fig. 6 Simulation of repaglinide drug-drug interactions with inhibitor drugs. Repaglinide oral mean plasma concentration-time curves when dosed alone or in combination with (**a**) OATP inhibitor – 100 mg cyclosporine, and (**b**) CYP and/or OATP inhibitors – 100 mg itraconazole and 600 mg gemfibrozil. Data points represent mean observed plasma concentration-time profiles of repaglinide when dosed alone (*open*) and in the presence of inhibitor drugs (*filled*) (32,35,36,39). For simulations, dosage regimen of the inhibitor drugs and repaglinide is similar to the original reported study design. Curves represent model simulations of mean plasma concentration-time profiles of repaglinide when dosed alone (*solid lines*) and in the presence of inhibitor drugs (*dashed lines*).

clearance, while keeping fm_{CYP2C8} constant (Figure 4). The current mechanistic model considers permeability-limited hepatic disposition and, therefore, the overall hepatic intrinsic clearance of repaglinide is expressed as: (28)

$$CL_{int,overall} = CL_{int,uptake} \times \frac{CL_{int,met}}{CL_{pd} + CL_{int,met}}$$

When the metabolic intrinsic clearance is greater than passive diffusion, the overall hepatic clearance is primarily determined by $CL_{int,uptake}$, and thus a change in the $CL_{int,met}$ would not significantly impact systemic exposure. On the contrary, when passive diffusion is appreciable relative to $CL_{int,met}$, the overall hepatic clearance is affected by changes in the $CL_{int,met}$. Increased repaglinide AUC ratios with decreased $CL_{int,met}$ is presumably due to gradual shift in the dependence of overall hepatic clearance on uptake clearance to a combination of uptake and metabolic clearance. Collectively, for drugs with permeability-limited hepatic disposition, both metabolic fraction and the intrinsic clearances are critical input parameters for quantitative DDI predictions.

While gemfibrozil and gemfibrozil 1-*O*-β-glucuronide exert a reversible inhibitory effect on OATP1B1, their relative contributions to the observed repaglinide-gemfibrozil DDI can be estimated using the ratio of the unbound plasma concentration [Iu] to *in vitro* unbound Ki values (Ki,u) (6). Both gemfibrozil and its metabolite showed ratio much above

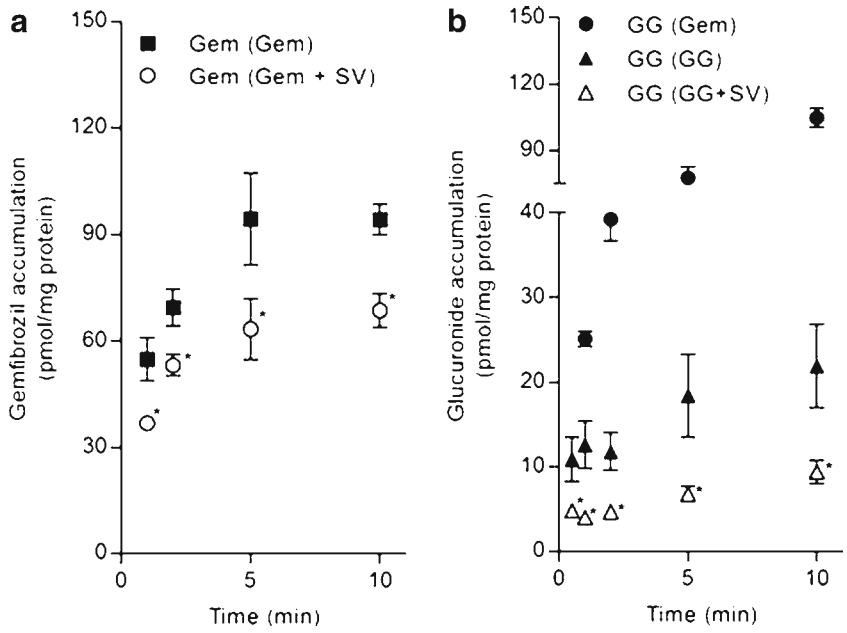

Fig. 7 Transport characteristics of gemfibrozil (Gem) and gemfibrozil 1-*O*-β-glucuronide (GG) in the sandwich culture human hepatocyte model. Accumulation of (**a**) gemfibrozil and (**b**) glucuronide in the absence and presence of rifamycin SV was measured, following incubation with each separately.

0.1 for up to 6 h postdose, and generally both seem to be equally responsible for the overall OATP1B1 inhibition (Figure 3). On the other hand, simulations suggested more than 95% of *in vivo* CYP2C8 inhibition is associated with mechanism-based inactivation by gemfibrozil 1-*O*-β-glucuronide.

The *in vitro* estimated repaglinide fm_{CYP2C8} (~0.45–0.71) (11–13) was speculated to be lower than would be expected (>0.85) on the basis of a collection of clinical repaglinide-gemfibrozil DDI reports, wherein CYP2C8 inhibition was assumed as the major DDI mechanism (14,15). However, the current mechanistic model closely predicted repaglinide-gemfibrozil interactions with *in vitro* fm_{CYP2C8}. Therefore, the CYP2C8 contribution to repaglinide metabolism *in vivo* is likely similar to that consistently observed *in vitro*. Furthermore, the *in vitro* data substantiate the clinical findings that CYP3A4 also plays a key role in repaglinide elimination. For example, in healthy volunteers, about 66% of repaglinide dose was excreted as metabolite M2 (50), which is predominantly formed by CYP3A4 (13).

Repaglinide has been recommended by the USFDA and the EMA as the "sensitive" probe drug (AUC ratio >5) for assessing CYP2C8 and OATP1B1 inhibitory activity of the investigational drug (7,8). Similarly, gemfibrozil was suggested as strong inhibitor to assess CYP2C8 enzyme activity *in vivo*. Here we demonstrated lack of disconnect in the *in vitro* and *in vivo* fm_{CYP2C8}, which was previously thought (14,15). Evidently, the observed high magnitude of DDIs with gemfibrozil is only partially associated with CYP2C8 inhibition (Figure 4), suggesting repaglinide is not a sensitive probe substrate for assessing CYP2C8 activity. On the other hand, hepatic uptake is the rate-determining step in the systemic clearance of repaglinide, which is thought to be driven by OATP1B1 (17), and therefore, repaglinide can be used as OATP1B1 probe substrate (Supplementary Material Figure S3d). The current repaglinide and gemfibrozil models can be applied for prospective prediction of DDIs with marketed and investigational drugs. For example, cyclosporine 100 mg single dose resulted in about 2.4-fold increase in repaglinide systemic exposure, primarily due to OATP1B1 inhibition (32). However, current model predicted that AUC ratio may increase to ~5.5-fold with 600 mg cyclosporine, suggesting that in patients receiving immunosuppression therapy with cyclosporine (upto 600 mg continuous dosing) have a similar magnitude of DDI as noted with single or multiple gemfibrozil therapeutic doses. A drug interaction study with high dose of cyclosporine may provide further insight into the role of hepatic uptake transporters in the disposition of repaglinide and to further validate or refine the current model.

Clinical DDI and pharmacogenomic studies demonstrated an increase in the plasma exposure and often markedly enhanced and/or prolonged the blood glucose-lowering effect of repaglinide (17,18,34,39). Repaglinide lowers blood glucose levels by stimulating the release of insulin from the pancreas while interfering with the ATP-dependent potassium channels in the β-cell membrane. Due to non-hepatic target site pharmacology, the pharmacodynamic activity of repaglinide is increased by inhibitor drugs like cyclosporine and gemfibrozil. On the contrary, for liver-target drugs like statins with similar disposition features, these inhibitor drugs may lead to reduced pharmacological effects and increased adverse events such as rhabdomyolysis, due to decreased hepatic and increased systemic concentrations, respectively. This is exemplified by cerivastatin, which is transported by OATP1B1 and metabolized by CYP2C8 and CYP3A4 (16,51). Cerivastatin was withdrawn from the market in 2001 after adverse events, including deaths, were reported; and significant number of events directly correlated with the coadministration of gemfibrozil (1). Cerivastatin systemic exposure increased by about 5.6-fold when coadministered with gemfibrozil (52), presumably due to similar quantitative effects of gemfibrozil on cerivastatin disposition, as noted here with repaglinide-gemfibrozil interaction.

CONCLUSIONS

In conclusion, a comprehensive PBPK model of repaglinide was developed using *in vitro* transport and metabolic kinetics and a hepatic active uptake scaling factor, obtained by fitting to the intravenous plasma concentration-time profile. Simulations demonstrated the ability of the current model to predict repaglinide plasma concentration-time profiles and the magnitude of exposure change under several drug interaction situations, including the complex interactions with gemfibrozil. The mechanistic evaluation suggests that hepatic uptake is rate-determining in the systemic clearance of repaglinide; and inhibition of both OATP1B1 and CYP2C8 need to be considered for quantitative rationalization of repaglinide-gemfibrozil DDIs. Furthermore, when hepatic uptake is rate-determining in the disposition of victim drug, the quantitative prediction of DDIs is influenced both by the metabolic fraction and intrinsic clearances. Finally, this work laid out a step-wise model building process and demonstrated the utility of mechanistic PBPK modeling and simulations in evaluating and/or predicting complex transporter- and enzyme-based drug interactions.

ACKNOWLEDGMENTS AND DISCLOSURES

The authors would like to thank Drs. Larissa Balogh and Larry Tremaine for comments and insightful discussion on the content of this manuscript.

All authors are full-time employees of Pfizer Inc. Constructive suggestions by the reviewers during revision are greatly appreciated. The authors have no conflicts of interest that are directly relevant to this study.

REFERENCES

1. Farmer JA. Learning from the cerivastatin experience. Lancet. 2001;358:1383–5.
2. Fahmi OA, Maurer TS, Kish M, Cardenas E, Boldt S, Nettleton D. A combined model for predicting CYP3A4 clinical net drug-drug interaction based on CYP3A4 inhibition, inactivation, and induction determined *in vitro*. Drug Metab Dispos. 2008;36:1698–708.
3. Obach RS, Walsky RL, Venkatakrishnan K, Gaman EA, Houston JB, Tremaine LM. The utility of *in vitro* cytochrome P450 inhibition data in the prediction of drug-drug interactions. J Pharmacol Exp Ther. 2006;316:336–48.
4. Hinton LK, Galetin A, Houston JB. Multiple inhibition mechanisms and prediction of drug-drug interactions: status of metabolism and transporter models as exemplified by gemfibrozil-drug interactions. Pharm Res. 2008;25:1063–74.
5. Yoshida K, Maeda K, Sugiyama Y. Transporter-mediated drug–drug interactions involving OATP substrates: predictions based on *in vitro* inhibition studies. Clin Pharmacol Ther. 2012;91:1053–64.
6. Giacomini KM, Huang SM, Tweedie DJ, Benet LZ, Brouwer KL, Chu X, Dahlin A, Evers R, Fischer V, Hillgren KM, Hoffmaster KA, Ishikawa T, Keppler D, Kim RB, Lee CA, Niemi M, Polli JW, Sugiyama Y, Swaan PW, Ware JA, Wright SH, Yee SW, Zamek-Gliszczynski MJ, Zhang L. Membrane transporters in drug development. Nat Rev Drug Discov. 2010;9:215–36.
7. USFDA. Drug interaction studies - study design, data analysis, implications for dosing, and labeling recommendations. Center for Drug Evaluation and Research (CDER) (2012)
8. EMA. Guideline on the Investigation of Drug Interactions. Committee for Human Medicinal Products (CHMP) (2012)
9. Huang SM, Rowland M. The role of physiologically based pharmacokinetic modeling in regulatory review. Clin Pharmacol Ther. 2012;91:542–9.
10. Scott LJ. Repaglinide: a review of its use in type 2 diabetes mellitus. Drugs. 2012;72:249–72.
11. Bidstrup TB, Bjornsdottir I, Sidelmann UG, Thomsen MS, Hansen KT. CYP2C8 and CYP3A4 are the principal enzymes involved in the human *in vitro* biotransformation of the insulin secretagogue repaglinide. Br J Clin Pharmacol. 2003;56:305–14.
12. Kajosaari LI, Laitila J, Neuvonen PJ, Backman JT. Metabolism of repaglinide by CYP2C8 and CYP3A4 *in vitro*: effect of fibrates and rifampicin. Basic Clin Pharmacol Toxicol. 2005;97:249–56.
13. Sall C, Houston JB, Galetin A. A comprehensive assessment of repaglinide metabolic pathways: impact of choice of *in vitro* system and relative enzyme contribution to *in vitro* clearance. Drug Metab Dispos. 2012;40:1279–89.
14. Honkalammi J, Niemi M, Neuvonen PJ, Backman JT. Dose-dependent interaction between gemfibrozil and repaglinide in humans: strong inhibition of CYP2C8 with subtherapeutic gemfibrozil doses. Drug Metab Dispos. 2011;39:1977–86.
15. Honkalammi J, Niemi M, Neuvonen PJ, Backman JT. Gemfibrozil is a strong inactivator of CYP2C8 in very small multiple doses. Clin Pharmacol Ther. 2012;91:846–55.
16. Niemi M, Leathart JB, Neuvonen M, Backman JT, Daly AK, Neuvonen PJ. Polymorphism in CYP2C8 is associated with reduced plasma concentrations of repaglinide. Clin Pharmacol Ther. 2003;74:380–7.
17. Niemi M, Backman JT, Kajosaari LI, Leathart JB, Neuvonen M, Daly AK, Eichelbaum M, Kivisto KT, Neuvonen PJ. Polymorphic organic anion transporting polypeptide 1B1 is a major determinant of repaglinide pharmacokinetics. Clin Pharmacol Ther. 2005;77:468–78.
18. Tornio A, Niemi M, Neuvonen PJ, Backman JT. Drug interactions with oral antidiabetic agents: pharmacokinetic mechanisms and clinical implications. Trends Pharmacol Sci. 2012;33:312–22.
19. Ogilvie BW, Zhang D, Li W, Rodrigues AD, Gipson AE, Holsapple J, Toren P, Parkinson A. Glucuronidation converts gemfibrozil to a potent, metabolism-dependent inhibitor of CYP2C8: implications for drug-drug interactions. Drug Metab Dispos. 2006;34:191–7.
20. Shitara Y, Hirano M, Sato H, Sugiyama Y. Gemfibrozil and its glucuronide inhibit the organic anion transporting polypeptide 2 (OATP2/OATP1B1:SLC21A6)-mediated hepatic uptake and CYP2C8-mediated metabolism of cerivastatin: analysis of the mechanism of the clinically relevant drug-drug interaction between cerivastatin and gemfibrozil. J Pharmacol Exp Ther. 2004; 311:228–36.
21. Fujino H, Shimada S, Yamada I, Hirano M, Tsunenari Y, Kojima J. Studies on the interaction between fibrates and statins using human hepatic microsomes. Arzneimittelforschung. 2003; 53:701–7.
22. Bi YA, Kazolias D, Duignan DB. Use of cryopreserved human hepatocytes in sandwich culture to measure hepatobiliary transport. Drug Metab Dispos. 2006;34:1658–65.
23. Rodgers T, Rowland M. Physiologically based pharmacokinetic modelling 2: predicting the tissue distribution of acids, very weak bases, neutrals and zwitterions. J Pharm Sci. 2006;95:1238–57.
24. Rodgers T, Leahy D, Rowland M. Physiologically based pharmacokinetic modeling 1: predicting the tissue distribution of moderate-to-strong bases. J Pharm Sci. 2005;94:1259–76.
25. Varma MV, Lai Y, Feng B, Litchfield J, Goosen TC, Bergman A. Physiologically based modeling of pravastatin transporter-mediated hepatobiliary disposition and drug-drug interactions. Pharm Res. 2012;29:2860–73.
26. Jones HM, Barton HA, Lai Y, Bi YA, Kimoto E, Kempshall S, Tate SC, El-Kattan A, Houston JB, Galetin A, Fenner KS. Mechanistic pharmacokinetic modeling for the prediction of transporter-mediated disposition in humans from sandwich culture human hepatocyte data. Drug Metab Dispos. 2012;40:1007–17.
27. Kilford PJ, Stringer R, Sohal B, Houston JB, Galetin A. Prediction of drug clearance by glucuronidation from *in vitro* data: use of combined cytochrome P450 and UDP-glucuronosyltransferase cofactors in alamethicin-activated human liver microsomes. Drug Metab Dispos. 2009;37:82–9.
28. Shitara Y, Horie T, Sugiyama Y. Transporters as a determinant of drug clearance and tissue distribution. Eur J Pharm Sci. 2006;27:425–46.
29. Gertz M, Harrison A, Houston JB, Galetin A. Prediction of human intestinal first-pass metabolism of 25 CYP3A substrates from *in vitro* clearance and permeability data. Drug Metab Dispos. 2010;38:1147–58.
30. Hatorp V, Oliver S, Su CA. Bioavailability of repaglinide, a novel antidiabetic agent, administered orally in tablet or solution form or intravenously in healthy male volunteers. Int J Clin Pharmacol Ther. 1998;36:636–41.
31. Skerjanec A, Wang J, Maren K, Rojkjaer L. Investigation of the pharmacokinetic interactions of deferasirox, a once-daily oral iron chelator, with midazolam, rifampin, and repaglinide in healthy volunteers. J Clin Pharmacol. 2010;50:205–13.
32. Kajosaari LI, Niemi M, Neuvonen M, Laitila J, Neuvonen PJ, Backman JT. Cyclosporine markedly raises the plasma concentrations of repaglinide. Clin Pharmacol Ther. 2005;78:388–99.

33. Niemi M, Neuvonen PJ, Kivisto KT. The cytochrome P4503A4 inhibitor clarithromycin increases the plasma concentrations and effects of repaglinide. Clin Pharmacol Ther. 2001;70:58–65.
34. Honkalammi J, Niemi M, Neuvonen PJ, Backman JT. Mechanism-based inactivation of CYP2C8 by gemfibrozil occurs rapidly in humans. Clin Pharmacol Ther. 2011;89:579–86.
35. Tornio A, Niemi M, Neuvonen M, Laitila J, Kalliokoski A, Neuvonen PJ, Backman JT. The effect of gemfibrozil on repaglinide pharmacokinetics persists for at least 12 h after the dose: evidence for mechanism-based inhibition of CYP2C8 *in vivo*. Clin Pharmacol Ther. 2008;84:403–11.
36. Hatorp V, Hansen KT, Thomsen MS. Influence of drugs interacting with CYP3A4 on the pharmacokinetics, pharmacodynamics, and safety of the prandial glucose regulator repaglinide. J Clin Pharmacol. 2003;43:649–60.
37. Marbury TC, Ruckle JL, Hatorp V, Andersen MP, Nielsen KK, Huang WC, Strange P. Pharmacokinetics of repaglinide in subjects with renal impairment. Clin Pharmacol Ther. 2000;67:7–15.
38. Niemi M, Backman JT, Neuvonen M, Neuvonen PJ, Kivisto KT. Rifampin decreases the plasma concentrations and effects of repaglinide. Clin Pharmacol Ther. 2000;68:495–500.
39. Niemi M, Backman JT, Neuvonen M, Neuvonen PJ. Effects of gemfibrozil, itraconazole, and their combination on the pharmacokinetics and pharmacodynamics of repaglinide: potentially hazardous interaction between gemfibrozil and repaglinide. Diabetologia. 2003;46:347–51.
40. VandenBrink BM, Foti RS, Rock DA, Wienkers LC, Wahlstrom JL. Evaluation of CYP2C8 inhibition *in vitro*: utility of montelukast as a selective CYP2C8 probe substrate. Drug Metab Dispos. 2011;39:1546–54.
41. Nakagomi-Hagihara R, Nakai D, Tokui T, Abe T, Ikeda T. Gemfibrozil and its glucuronide inhibit the hepatic uptake of pravastatin mediated by OATP1B1. Xenobiotica. 2007;37:474–86.
42. Guest EJ, Rowland-Yeo K, Rostami-Hodjegan A, Tucker GT, Houston JB, Galetin A. Assessment of algorithms for predicting drug-drug interactions via inhibition mechanisms: comparison of dynamic and static models. Br J Clin Pharmacol. 2011;71:72–87.
43. Zhao P, Vieira Mde L, Grillo JA, Song P, Wu TC, Zheng JH, Arya V, Berglund EG, Atkinson Jr AJ, Sugiyama Y, Pang KS, Reynolds KS, Abernethy DR, Zhang L, Lesko LJ, Huang SM. Evaluation of exposure change of nonrenally eliminated drugs in patients with chronic kidney disease using physiologically based pharmacokinetic modeling and simulation. J Clin Pharmacol. 2012;52:91S–108S.
44. Watanabe T, Kusuhara H, Maeda K, Shitara Y, Sugiyama Y. Physiologically based pharmacokinetic modeling to predict transporter-mediated clearance and distribution of pravastatin in humans. J Pharmacol Exp Ther. 2009;328:652–62.
45. Kimoto E, Yoshida K, Balogh LM, Bi YA, Maeda K, El-Kattan A, *et al*. Characterization of Organic Anion Transporting Polypeptide (OATP) expression and its functional contribution to the uptake of substrates in human hepatocytes. Mol Pharm. 2012.
46. Knauer MJ, Urquhart BL, Meyer zu Schwabedissen HE, Schwarz UI, Lemke CJ, Leake BF, Kim RB, Tirona RG. Human skeletal muscle drug transporters determine local exposure and toxicity of statins. Circ Res. 2010;106:297–306.
47. Varma MV, Rotter CJ, Chupka J, Whalen KM, Duignan DB, Feng B, Litchfield J, Goosen TC, El-Kattan AF. pH-sensitive interaction of HMG-CoA reductase inhibitors (statins) with organic anion transporting polypeptide 2B1. Mol Pharm. 2011;8:1303–13.
48. Shitara Y, Takeuchi K, Nagamatsu Y, Wada S, Sugiyama Y, Horie T. Long-lasting inhibitory effects of cyclosporin A, but not tacrolimus, on OATP1B1- and OATP1B3-mediated uptake. Drug Metab Pharmacokinet. 2012.
49. Amundsen R, Christensen H, Zabihyan B, Asberg A. Cyclosporine A, but not tacrolimus, shows relevant inhibition of organic anion-transporting protein 1B1-mediated transport of atorvastatin. Drug Metab Dispos. 2010;38:1499–504.
50. van Heiningen PN, Hatorp V, Kramer Nielsen K, Hansen KT, van Lier JJ, De Merbel NC, Oosterhuis B, Jonkman JH. Absorption, metabolism and excretion of a single oral dose of (14)C-repaglinide during repaglinide multiple dosing. Eur J Clin Pharmacol. 1999;55:521–5.
51. Boberg M, Angerbauer R, Fey P, Kanhai WK, Karl W, Kern A, Ploschke J, Radtke M. Metabolism of cerivastatin by human liver microsomes *in vitro*. Characterization of primary metabolic pathways and of cytochrome P450 isozymes involved. Drug Metab Dispos. 1997;25:321–31.
52. Backman JT, Kyrklund C, Neuvonen M, Neuvonen PJ. Gemfibrozil greatly increases plasma concentrations of cerivastatin. Clin Pharmacol Ther. 2002;72:685–91.
53. Plum A, Muller LK, Jansen JA. The effects of selected drugs on the *in vitro* protein binding of repaglinide in human plasma. Methods Find Exp Clin Pharmacol. 2000;22:139–43.
54. Varma MV, Obach RS, Rotter C, Miller HR, Chang G, Steyn SJ, El-Kattan A, Troutman MD. Physicochemical space for optimum oral bioavailability: contribution of human intestinal absorption and first-pass elimination. J Med Chem. 2010;53:1098–108.
55. Albaugh D, Farrell T, Langan M, Lai WG. High throughput quantitative assessment of CYP inactivation using 2 concentration points. Drug Metab Lett. 2009;3:78–82.
56. Polasek TM, Miners JO. Quantitative prediction of macrolide drug-drug interaction potential from *in vitro* studies using testosterone as the human cytochrome P4503A substrate. Eur J Clin Pharmacol. 2006;62:203–8.